Computer simulation study of liquid CH_2F_2 with a new effective pair potential model

Pál Jedlovszky[a),b)] and Mihaly Mezei
Department of Physiology and Biophysics, Mount Sinai School of Medicine, New York, New York 10029

(Received 14 September 1998; accepted 5 November 1998)

A new effective pair potential model is proposed for computer simulations of liquid methylene fluoride and used in Monte Carlo simulations on the isothermal-isobaric ensemble at two different temperatures. The new model is able to reproduce the thermodynamic (internal energy, density, heat capacity, vapor-liquid equilibrium) and structural (neutron diffraction data) properties of liquid methylene fluoride with good accuracy. The structure of liquid methylene fluoride is analyzed in detail on the basis of the present simulation at 153 K. It is found that, unlike in liquid water, the preferential location of the nearest neighbors is in the direction of the face centers of the tetrahedron of the central molecule. However, the four nearest neighbors do not surround the central molecule in a highly tetrahedral arrangement: the obtained distribution of the tetrahedral angular order parameter is rather similar to that in liquid argon. Preferential head-to-tail type orientation is found for nearest neighbors, accompanied by a slight preference for antiparallel dipole–dipole arrangement. The orientational correlation of the molecules is found to be rather long ranged, extending over the first coordination shell. The observed preferential nearest neighbor arrangement is resulted from the competition of steric and electrostatic interactions. No evidence for C–H$\cdots$F type hydrogen bonding is found in liquid methylene fluoride. © *1999 American Institute of Physics.* [S0021-9606(99)51506-7]

I. INTRODUCTION

Chlorofluorocarbon compounds, such as $CHClF_2$ or CCl_2F_2 has been widely used as refrigerants in the past decades. However, due to their ability of forming chlorine radicals, these molecules have a destructive effect on the stratospheric ozone layer, and therefore their industrial use have been limited by the Montreal Protocol of 1987. Due to their thermodynamic properties hydrofluorocarbons are possible environmentally friendly alternatives of chlorofluorocarbon refrigerants, and thus there is a rapidly increasing interest of modeling the thermodynamics of such compounds in detail. For this purpose, numerous potential models have been developed and used in computer simulations.[1–7]

Besides their thermodynamic properties the liquid structure of these compounds is also very important from a theoretical point of view. The ability of the CH group of participating in hydrogen bonds have been intensively studied in various systems.[8–12] Due to their small molecular size and the large electronegativity of the F atom, hydrofluoromethanes are very good candidates for studying the possible formation of such C–H$\cdots$F hydrogen bonds. Moreover, the CH_2F_2 molecule has the same C_{2v} symmetry as water, and thus its molecular geometry can even enable methylene fluoride to form extensive tetrahedral water-like network. However, besides this possible ability of forming weak hydrogen bonds, there are other factors which can also play important role in determining the molecular structure of liquid CH_2F_2. The experimental gas-phase dipole moment of the CH_2F_2 molecule (1.98D, see Appendix D of Ref. 13) is unusually large, and thus strong dipole–dipole interactions can also be expected in the liquid phase. Steric interactions can also be very important in forming the liquid structure, since this interaction has been found to be the most important factor in determining the structure of various dipolar liquids.[14] Beyond its theoretical importance, the competition of these three interactions in forming the liquid structure can also be reflected in the thermodynamic behavior of methylene fluoride, and thus the understanding of the liquid structure can also be a great help in the investigation of suitable substitutes of chlorofluorocarbon compounds.

The aim of the present study is to analyze the intermolecular structure of liquid methylene fluoride in detail with computer simulation and investigate the possible structure determining role of the various (i.e., C–H$\cdots$F type hydrogen bonding, dipolar, and steric) interactions. For this purpose, an existing potential model[7] of liquid CH_2F_2 has been modified in order to get a better reproduction of structural[15] and thermodynamic[16] properties of the liquid. The structure obtained from the simulation has then been analyzed in terms of pair correlation functions, orientational correlation and spatial distribution of the molecules. The obtained results are compared to that of other liquids of the C_{2v} symmetry group, such as water, a liquid where the structure is mainly determined by the hydrogen bonding interactions,[17] H_2S, in which steric interactions are by far the most important ones,[18] and methylene chloride where the competition of dipolar and steric interactions determines the liquid structure.[19]

a)Corresponding author; electronic mail: pali@inka.mssm.edu
b)On leave from: Central Research Institute for Chemistry of the Hungarian Academy of Sciences, Budapest, Hungary.

This paper is organized as follows. In Sec. II the applied potential model is described, in Sec. III details of the Monte Carlo simulations are given, whereas in Secs. IV and V the obtained thermodynamical and structural results are discussed in detail. Finally, in Sec. VI some conclusions are drawn.

II. POTENTIAL MODEL

Despite its importance both from theoretical and industrial point of view, liquid methylene fluoride attracted relatively little interest until recently. To our knowledge, neither computer simulations nor diffraction experiments have been performed on this liquid before the mid-nineties. However, in 1997 development of two different effective pair potentials were reported.[6,7] The Higashi-Takada (HT) model[6] is rigid, the intermolecular interactions are described by Coulombic and Lennard-Jones interactions between the atomic sites. The molecular geometry and the fractional charges used in this model have been determined by *ab initio* calculations and the Lennard-Jones parameters have been fitted to the experimental vapor-liquid equilibrium properties. However, the results obtained with this model in the liquid state (e.g., internal energy, density, pair correlation functions, etc.) have not been compared with experimental data. The Potter–Tildesley–Burgess–Rogers (PTBR) model[7] describes the intermolecular interactions in a similar way, but, contrary to the HT model, the Lorentz–Berthelot combining rules of the Lennard-Jones parameters have not been applied here for the H–F atom pairs. The PTBR model is semiflexible: it uses rigid bond lengths and flexible harmonic bond angles. The model can reproduce experimental thermodynamic properties reasonably well. However, the total neutron diffraction pair correlation function obtained with this model deviates from the experimental curve[15] in some points. Among these deviations, the most important one is that the PTBR model predicts the position of the first (negative) peak at about 0.2 Å smaller r values than the experimental finding. Since this peak can be associated with the nearest H–F pairs, its accurate description is essential for a reliable modeling of the short range intermolecular structure of the liquid. Therefore, we have modified the PTBR model slightly by applying the Lorentz–Berthelot combining rule also for the H–F Lennard-Jones interactions in order to correct this deviation. We have further simplified the model by using rigid molecules, setting the bond angles equal to their equilibrium values in the PTBR model. Thus the C–H and C–F bond lengths and the H–C–H and F–C–F bond angles have been set to 1.09, 1.36 Å, 113.61°, and 108.63° in this model, respectively. Finally, the fractional charges have been slightly modified in order to get a better reproduction of the internal energy and density of the liquid at 153 and 221.5 K at atmospheric pressure. The used fractional charges and Lennard-Jones parameters are summarized in Table I.

TABLE I. Fractional charges and Lennard-Jones parameters of the used potential model.

	q/e	σ/Å	ϵ/K
C	+0.300	3.150	54.6
H	+0.075	2.170	10.0
F	−0.225	2.975	40.0

The dimer potential energy surface of this model has two distinct minima. The geometries corresponding to these minima are shown in Fig. 1. The global minimum of the energy surface is −5.952 kJ/mol, corresponding to the dimer geometry labeled A in Fig. 1. In this arrangement, the molecules have three H–F atom pairs in close contact, separated by 2.6 Å each, and thus it is favorable for the charge–charge interactions. The angle between the dipole moment of the two molecules is 106°, indicating that quadrupolar forces can play a more important role in the determination of this dimer arrangement than dipole–dipole interaction. The geometry labeled B corresponds to a local minimum of −5.124 kJ/mol of the dimer potential energy surface. This arrangement, where the two dipole vectors are in antiparallel alignment, is very similar to the usual minimum energy configuration of dimers of aprotic dipolar molecules, such as acetone, acetonitrile, pyridine, etc.[14] In this dimer, there are four H–F contacts at 2.7 Å, involving H atoms which are bifurcated between the two F atoms of the other molecule. Although both dimers have several H–F contacts, the corresponding C–H$\cdots$F angles are rather far from being linear, they are about 112° in dimer A and 120° in dimer B. Since these geometries are rather far from the typical linear hydrogen bonding angles, it can be concluded that the energy minimum arrangements of the methylene fluoride dimer contain no or only very distorted C–H$\cdots$F hydrogen bonds.

III. COMPUTER SIMULATIONS

Two Monte Carlo simulations have been performed on the isothermal-isobaric ensemble with 512 CH_2F_2 molecules at 10^5 Pa. The simulation temperatures were 153 and 221.5 K, the latter being the boiling temperature at this pressure. Cubic simulation box and standard periodic boundary conditions have been used. The long-range part of the electrostatic interactions has been taken into account by the reaction field correction method,[20,21] and thus the interaction energy of two particles have been evaluated through the formula

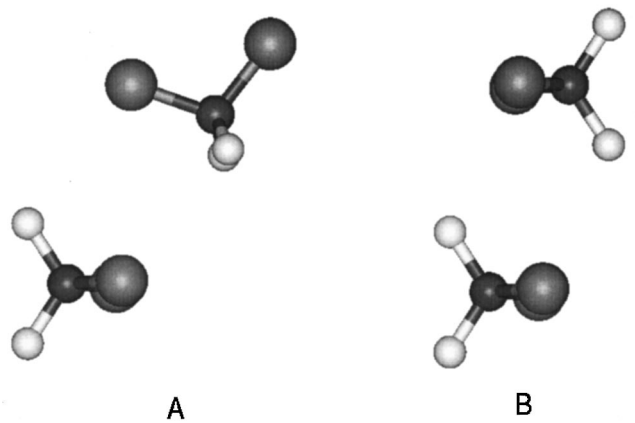

FIG. 1. Configurations of the CH_2F_2 dimer corresponding to minima of the dimer potential energy surface of the present model. A: global minimum configuration with interaction energy of −5.95 kJ/mol. B: configuration corresponding to a local minimum with interaction energy of −5.12 kJ/mol.

TABLE II. Thermodynamic properties of liquid methylene fluoride as obtained from simulations with different potential models.

		U/kJ mol^{-1}	U_{LJ}/kJ mol^{-1}	U_C/kJ mol^{-1}	ρ/g cm^{-3}	C_p/J mol^{-1} K^{-1}
Present model		-21.32 ± 0.12	-11.39 ± 0.10	-9.93 ± 0.10	1.407 ± 0.011	76.58
PTBR	153.0 K	-20.03 ± 0.16	-12.17 ± 0.09	-11.09 ± 0.09	1.552 ± 0.010	84.77
HT		-23.07 ± 0.13	-13.98 ± 0.10	-9.09 ± 0.07	1.391 ± 0.008	72.18
Experiment		-22.03[a]			1.403[b]	81.82[a]
Present model		-17.40 ± 0.20	-9.27 ± 0.12	-8.13 ± 0.10	1.199 ± 0.014	76.69
PTBR	221.5 K	-14.87 ± 0.24	-10.15 ± 0.13	-9.34 ± 0.12	1.332 ± 0.013	95.23
HT		-19.20 ± 0.19	-11.67 ± 0.13	-7.54 ± 0.10	1.213 ± 0.010	62.50
Experiment		18.03[a]			1.215[c]	82.57[a]

[a]Obtained from the Tillner–Roth–Yokozeki equation of state (see Ref. 16).
[b]Reference 7.
[c]Reference 23, value obtained with extrapolation.

$$U_{ij}=\sum_{\alpha=1}^{5}\sum_{\beta=1}^{5}\frac{1}{4\pi\in_0}\frac{q_\alpha q_\beta}{r_{i\alpha,j\beta}}\left[1+\frac{\in_{RF}-1}{2\in_{RF}+1}\left(\frac{r_{i\alpha,j\beta}}{R_C}\right)^3\right]+4\epsilon_{\alpha\beta}\left[\left(\frac{\sigma_{\alpha\beta}}{r_{i\alpha,j\beta}}\right)^{12}-\left(\frac{\sigma_{\alpha\beta}}{r_{i\alpha,j\beta}}\right)^{6}\right], \quad (1)$$

if the distance of their C atoms were smaller than $R_C=15$ Å, and have been set to zero otherwise. In this equation, indices α and β run through the five atomic sites of molecule i and j, respectively, $r_{i\alpha,j\beta}$ is the distance of site α on molecule i and site β on molecule j, $\in_0$ is the vacuum permittivity, $\in_{RF}$ is the dielectric constant of the continuum beyond the interaction truncation distance of R_C (in this study its value has been set to infinity), q_α and q_β are the fractional charges on sites α and β, respectively, and $\epsilon_{\alpha\beta}$ and $\sigma_{\alpha\beta}$ are the Lennard-Jones interaction parameters, which have been obtained from ϵ_α and ϵ_β and from σ_α and σ_β by the Lorentz–Berthelot combining rules [i.e., $\epsilon_{\alpha\beta}=(\epsilon_\alpha\epsilon_\beta)^{1/2}$ and $\sigma_{\alpha\beta}=(\sigma_\alpha+\sigma_\beta)/2$]. The energy of the Lennard-Jones interaction of particles beyond R_C have been estimated by assuming that all of the partial pair correlation functions are equal to unity in this region.[22]

In the simulations, every 512 particle displacement step have been followed by a volume change step. Systems have been equilibrated by 5 million particle displacement steps. Thermodynamic properties and pair correlation functions have been averaged over 20000 equilibrium configurations, separated by 512 particle displacement steps each. In the 153 K simulation, 100 equilibrium configurations, separated by 256 000 particle displacement steps each, have been saved for detailed structural analysis. For comparisons, simulations with the HT and PTBR models have also been performed under the same conditions.

IV. THERMODYNAMIC RESULTS

A. Liquid properties

The most important thermodynamic properties of liquid CH_2F_2 at 153 and 221.5 K are summarized in Table II as obtained from the present simulations. For comparisons, results obtained with the PTBR and HT models as well as experimental data are also shown. As is apparent, the PTBR model underestimates the magnitude of the U potential energy by about 9% and 17% at 153 and 221.5 K, respectively. Moreover, it overestimates the density of the liquid at both temperatures by 10%. The results obtained with the HT model are considerably better, this model can reproduce the liquid density very well, within 1%, whereas it results in about 5%–6% lower potential energy than the experimental data at both temperatures. The best agreement with these experimental data is obtained with the present model, which can reproduce the potential energy and the density of the liquid within 3.5% and about 1%, respectively, at both temperatures. The C_p heat capacity of the system has also been calculated from the different simulations and compared with experimental data in Table II. The kinetic part of the heat capacity have been estimated as $3/R$, whereas its configurational part have been calculated from the fluctuation of the enthalpy,[22] and thus it could be determined with considerably lower accuracy than the energy or the density. At 153 K the best result is obtained with the PTBR model, which reproduced the experimental value within 4%. However, at 221.5 K it deviates from the experimental data by about 15%. The present model reproduces the experimental value within 6–7 % at both temperatures, whereas in reproducing the heat capacity of the system the HT model proved to be the least accurate among the three models tested here.

In order to investigate the relative importance of the Coulombic and dispersion interactions in the energetics of liquid CH_2F_2, we have also calculated the separate contributions of the Lennard-Jones and Coulombic terms (U_{LJ} and U_{C}, respectively) to the total potential energy of the system. These values are also included in Table II. Although such a separation of the different energy terms is rather arbitrary in the case of an effective potential model, the fact that the Coulombic and Lennard-Jones terms are of similar magnitude at both temperatures with all the three different potential models indicates that the energetics of liquid CH_2F_2 is not dominated simply by one kind of interaction.

For investigating the possible presence of hydrogen bonds, we have determined the distribution of the U_{ij} pair interaction energies. The distributions obtained at 153 and 221.5 K are shown in Fig. 2. Both curves have a well-defined shoulder at -5 kJ/mol, on the attractive side of the main trivial peak of the noninteracting molecular pairs. The presence of this shoulder is a clear sign of the association of the

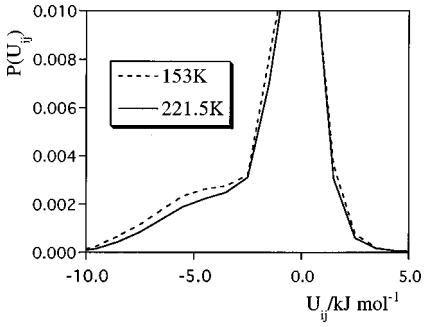

FIG. 2. Distribution of the U_{ij} pair interaction energy of the methylene fluoride molecules at two different temperatures as obtained from simulations with the present potential model.

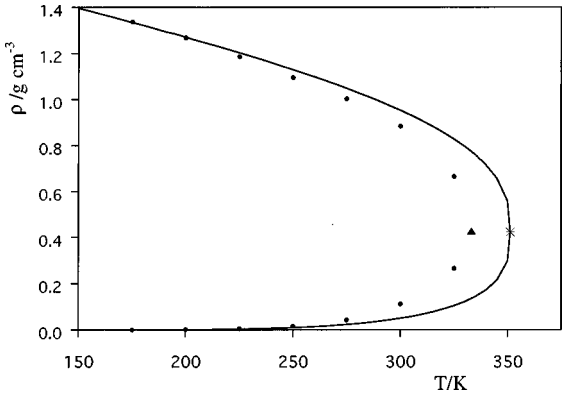

FIG. 3. Vapor-liquid equilibrium densities of liquid methylene fluoride as a function of the temperature. The solid curve is obtained from the Tillner–Roth–Yokozeki equation of state (see Ref. 16), the asterisk is the experimental critical point, dots are the results of the cavity biased Gibbs ensemble Monte Carlo simulations with the present model, and the triangle is the estimated critical point of the model.

molecules. This association can be weak C–H···F type hydrogen bonding, association involving more than one H–F contacts (e.g., dimer A of Fig. 1), or simply dipolar association, such as dimer B of Fig. 1 or any kind of head-to-tail type arrangement. Similar shoulder appears on the $P(U_{ij})$ distribution of liquid formic acid as a result of the C–H···O type hydrogen bonds[11] and on that of liquid acetone[24] and acetonitrile[25] due to the dipolar association of the molecules. However, the integration of the obtained shoulder up to -2.5 kJ/mol reveals that the molecules have about six strongly associated neighbors at both temperatures. This value is considerably larger than the largest possible number of hydrogen bonded neighbors, which suggests that C–H···F type hydrogen bonding cannot be the dominant form of the molecular association in liquid methylene fluoride.

B. Vapor-liquid equilibrium

The vapor-liquid equilibrium properties of liquid methylene fluoride have been investigated using the Gibbs ensemble Monte Carlo method[26] with cavity-biased particle insertion.[27] In these simulations, the temperature and the overall density of the two systems have been fixed (i.e., the sum of the two cell's volume and the sum of the number of particles in the two cells remained constant during the simulation). Simulations have been performed at seven different temperatures, namely at 175, 200, 225, 250, 275, 300, and 325 K. The two cubic simulation boxes have contained 513 molecules altogether. Molecule transfers have been attempted after every pair of displacement steps, and volume exchange steps have been performed after every 500 displacement attempt pairs. Particle insertions have been tried into cavities of radius fluctuating around 3 Å, with the exception of the 325 K run. In the 325 K simulation, there was no need for cavity biasing because of the relatively low density of the liquid phase at this temperature. The maximum translation and rotation of a particle in the displacement steps have been 0.3 Å and 15°, respectively, and the maximum change of the box volume in one step has been 400 Å.[3] In the equilibration phase of the simulations 5 million, in the production phase 10 million pairs of particle displacement steps have been performed.

The obtained coexisting densities of the liquid and vapor phase are shown in Fig. 3 as a function of the temperature. For comparison, the phase diagram obtained with the Tillner–Roth–Yokozeki equation of state[16] is also plotted here. The obtained agreement with the equation of state curve is rather satisfactory, it is generally somewhat better than that of the original PTBR model (see Fig. 2 of Ref. 7). The present model reproduces very well the experimental curve at temperatures below 275 K, whereas the PTBR model works somewhat better around 300 K for the liquid phase. However, as far as the vapor density is concerned the two models work with about the same level of accuracy, resulting in increasing deviation from the experimental curve with increasing temperature.

Obviously, it cannot be expected that an effective pairwise additive potential model reproduces accurately the coexisting liquid and vapor phase densities over a broad temperature range. The parameters of the present model have been optimized to the thermodynamic properties (including the density) of liquid methylene fluoride at 153 and 221.5 K, and thus it is not surprising that it can reproduce this part of the phase diagram with the best accuracy. However, in spite of the increasing deviation form the experimental curve at the high temperature region, the present model reproduces the experimental critical point ($T_c^{\mathrm{exp}}=351.3\,\mathrm{K}$, $\rho_c^{\mathrm{exp}}=0.424\,\mathrm{g/cm^3}$) rather accurately. The critical temperature and density of the model ($T_c^{\mathrm{model}}=333\,\mathrm{K}$, $\rho_c^{\mathrm{model}}=0.427\,\mathrm{g/cm^3}$), estimated by fitting a fourth-order polynomial to the simulated points above 250 K, agree with the experimental data within 5% and within 1%, respectively, which is considerably better than what has been obtained with the PTBR model.[7] This surprisingly good reproduction of the critical point by the present model is a consequence that (i) the model can reproduce the curvature of the experimental phase diagram, even if the actual density values are deviating from it at high temperature, and (ii) the deviation of the simulated liquid and vapor densities from the experimental curve in this region are roughly equal.

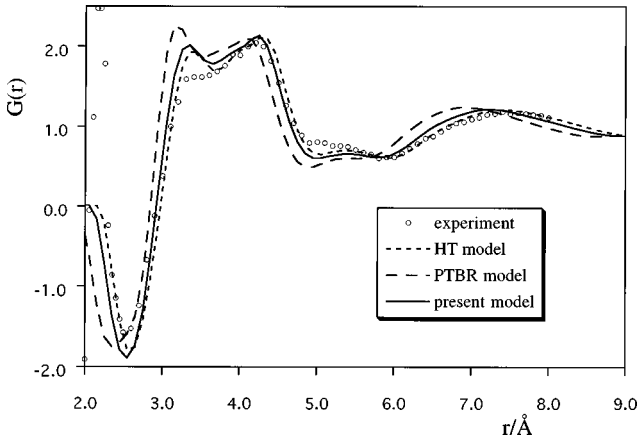

FIG. 4. Comparison of the experimental total neutron diffraction pair correlation function of liquid CH_2F_2 with that obtained from simulations with different potential models at 153 K.

V. STRUCTURAL RESULTS

A. Pair correlation functions

Besides the thermodynamic results the present potential model should also be tested against experimental structural data of liquid CH_2F_2. To our knowledge, only one diffraction experiment has been performed on this liquid so far,[15] namely, a neutron diffraction measurement at 153 K on a sample containing light hydrogen atoms. The obtained $G(r)$ total pair correlation function can directly be compared with simulation results as $G(r)$ is a linear combination of the six $g_{ij}(r)$ partial pair correlation functions with the weights

$$w_{ij}=\frac{(2-\delta_{ij})x_i x_j b_i b_j}{(\Sigma_{i=1}^{3} x_i b_i)^2}. \tag{2}$$

Here x_i is the mole fraction of atom type i in the sample (i.e., $x_C=0.2$ and $x_H=x_F=0.4$), δ_{ij} is the Kronecker delta function and b_i is the coherent neutron scattering amplitude of the i type nucleus. The $G(r)$ function obtained from the 153 K simulation is compared with the experimental data in Fig. 4. The total pair correlation functions obtained from the simulations with the HT and the original PTBR model are also shown here. It is evident that the present modification of the PTBR model improved the reproduction of the experimental structural data considerably. The approximately 0.2 Å difference in the position of the first minimum between the experimental data and the PTBR results is now corrected. This minimum is of a great structural importance, since it comes from the close-contact H–F pairs, and thus it contains information on nearest neighbor arrangement and on the possible presence of hydrogen bonds in the system. The improvement of the position of this minimum is a direct consequence of the application of the Lorentz–Berthelot rule also for the H–F pairs. The overall reproduction of the experimental $G(r)$ function with the present model is fairly good, the only feature which is not reproduced well is the shoulder of the main peak at about 3.5 Å. However, even in this region, the model shows considerable improvement over the PTBR model as the position of the first shoulder is now correctly reproduced and the amplitude of the obtained peak at this position is also reduced. The obtained $G(r)$ does not differ considerably from that of the HT model. The good reproduction of the experimental neutron diffraction results and thermodynamic data supports the reliability of the following detailed structural analysis.

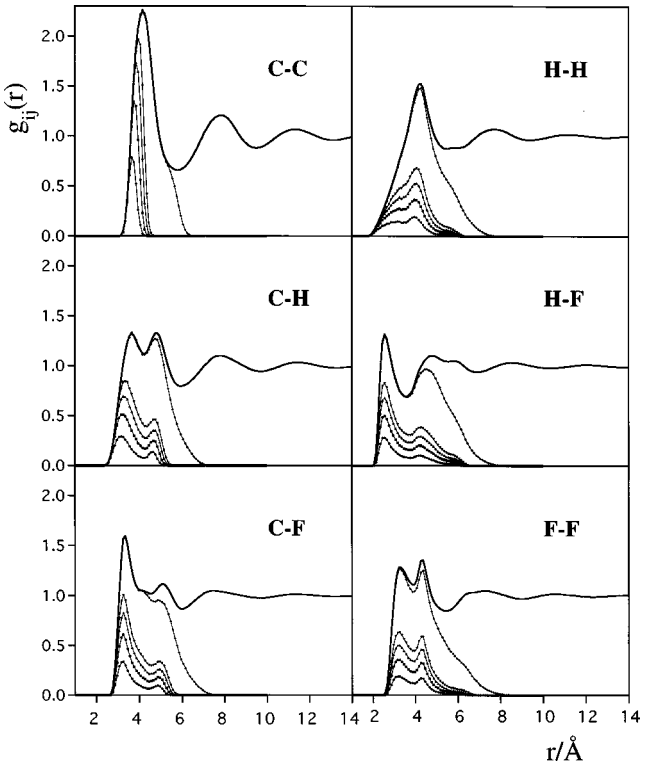

FIG. 5. Partial pair correlation functions of liquid methylene fluoride as obtained from the present simulation (solid lines). The contribution of the first one, two, three, four and thirteen neighbors are also shown.

The obtained six $g_{ij}(r)$ partial pair correlation functions are summarized in Fig. 5. The shape of the obtained functions are rather similar to that of liquid methylene chloride in general (see Fig. 4. of Ref. 19), indicating strong similarities in the structure of the two liquids. However, there are also some differences between the two structures, among which the most important one is indicated by the first peak of the two $g_{HX}(r)$ functions (being X the halogen atom). Namely, the first peak of the present $g_{HF}(r)$ function is much sharper and the following minimum is considerably deeper than that of $g_{HCl}(r)$ in liquid CH_2Cl_2. Moreover, the position of this peak and minimum (being at 2.55 and 3.55 Å, respectively) appear at about 0.5 Å lower r values here than in liquid methylene chloride, whereas the closest possible approach of the H and the halogen atom is about 2 Å in both liquids. Although this sharp rise of the first peak of $g_{HF}(r)$ on the low r side could be a sign of the presence of weak C–H$\cdots$F type hydrogen bonds, the descending part of the peak is much less sharp, here the function drops from about 1.3 to 0.7 in a 1 Å wide interval in contrast to the low r side rise from 0 to 1.3 within 0.5 Å. Moreover, the integration of the peak up the following minimum yields a H–F coordination number of 4.4, which is definitely too large to be consistent with a regular hydrogen bonding scheme.

The position of the first peak of the $g_{CF}(r)$ function, that is also a sign of the same nearest neighbor interaction, appears at 3.35 Å. This distance is about 0.3 Å smaller than the sum of the C–H bond length and the average close-contact H$\cdots$F distance [the first peak position of $g_{HF}(r)$], indicating that the C–H$\cdots$F angle of the close contact H–F pairs is considerably bent. The average value of this angle is estimated to be about 130° by the cosine rule.

The obtained $g_{HH}(r)$ function is rather similar to that of liquid methylene chloride.[19] Although the closest possible H–H contact is about 1.8 Å, the position of the first peak appears only at 4.25 Å. This very slow rise of the first peak of $g_{HH}(r)$, similarly to the case of liquid CH_2Cl_2, indicates the competition of the steric and electrostatic interactions in determining the liquid structure. Namely, the close contact of the small H atoms is preferable for the steric interactions, whereas it is clearly disfavorable to the electrostatic interactions due to the Coulombic repulsion. The shape of this peak suggests that nearest neighbors with both close H–H contact as well as with rather distant H atoms can be found in liquid methylene fluoride.

The $g_{CC}(r)$ pair correlation function shows all the features of a closely packed system. Similarly to liquid argon, the ratio of the second and first peak position (being at 7.85 and 4.15 Å, respectively) is about 1.9, the ratio of the first minimum and first peak position (the former being at 5.85 Å) is 1.4, and the coordination number of the first peak up to the following minimum is about 13. The integration of $g_{HH}(r)$ up to its first minimum and $g_{CH}(r)$, $g_{CF}(r)$, and $g_{FF}(r)$ up to their minimum following the splitted first peak yields similar values, indicating 11, 14, 14, and 10.5 molecules in the first coordination shell, respectively.

In order to investigate the relative arrangement of the nearest neighbor molecules in more detail we have also calculated the contribution of the first 1, 2, 3, 4, and 13 nearest neighbors to the six partial pair correlation functions. These contributions are also shown on Fig. 5. The distance of the neighbor molecules have been defined by their C–C distance. As is apparent, the contribution of the neighbors at different distances are rather similar to each other, and thus these neighbors, unlike in strongly hydrogen bonding liquids (e.g., HF[28]), are equivalent. With the exception of $g_{CC}(r)$, all contributions have two distinct peaks, the positions of which change negligibly with the C–C separation of the neighbor molecules. The positions of these peaks agree also well with the positions of the first and second peak of the full partial pair correlation function for C–H, C–F, H–F, and F–F atom pairs. The reason for this splitting is simply the fact that a molecular pair gives more than one contribution to these pair correlations. However, the picture is not so simple in the case of the H–H correlation, where this splitting of the nearest neighbors contribution can also be a sign of the existence of different nearest neighbor orientations. Here the nearest neighbors contribution has a peak around 3 Å, the region of the slow rise of the first peak of $g_{HH}(r)$. This peak is formed by neighbors in close H–H contact. To demonstrate this, we have recalculated the contributions of the first nearest neighbors to $g_{ij}(r)$, however, now the neighbors have been sorted according to the distance of their closest contact atom pairs instead of their C–C separation. The comparison of the two kind of nearest neighbor contributions are shown in Fig. 6 for H–H and H–F correlations. (For the other four atom pairs, the two kind of contributions do not differ considerably.) Now the first peak of the H–H contribution becomes much sharper and appears at about 1 Å lower r values than for the nearest C–C distance defined neighbors. Clearly this peak at 2.2 Å is coming from the molecular pairs with close H–H contact. Since no such peak appears on the contribution of the next (i.e., second, third, etc.) closest contact-defined neighbors, the relative importance of this kind of H–H contact neighbors is relatively small—a molecule has less than one such neighbor in average. The presence of this kind of close H–H contact neighbors have also been found in liquid methylene chloride,[19] even to a larger extent than here.

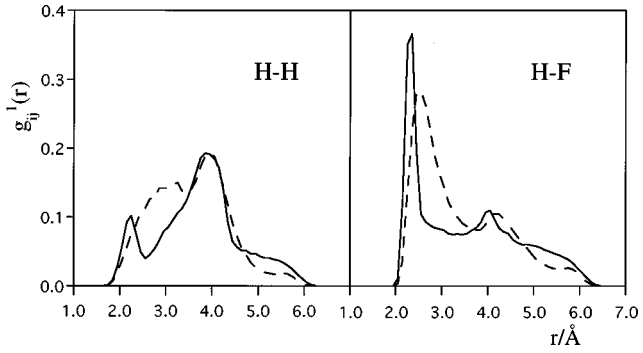

FIG. 6. Contribution of the first nearest neighbors to the H–H and H–F pair correlation function. Solid line: neighbor distance is defined by their closest contact atom pairs. Dashed line: neighbor distance is defined by their C–C separation.

When comparing the contributions of the nearest neighbors defined by their close contact and by their C–C distance to $g_{HF}(r)$, again a much sharper first peak is found for the close contact pairs. This sharp peak comes from the close H–F contact molecular pairs, whereas the second peak region of the function, covering partly the r range of the second peak of $g_{HF}(r)$, is mainly resulting from the noncontacting H–F pairs of these molecules.

B. Spatial distribution of the neighbors

The distribution of the neighboring molecules in the space around a central particle can be characterized by the cosine distribution of the θ angle formed by two neighbors around the central molecule. The θ angle is often referred as ''bond angle,'' although it is obviously not related to any chemical bonding. The $P(\cos\theta)$ distribution of liquid methylene fluoride is shown in Fig. 7 as resulted from the present simulation. In this analysis neighbors closer than 4.2 and 5.85 Å (according to their C–C distance) have been taken into account. These values correspond to the C–C coordination numbers of 4 and 13 (i.e., the entire first coordination shell), respectively. The obtained distributions have their main peak around 0.5 and a second peak at negative $\cos\theta$ values. This kind of $P(\cos\theta)$ distribution is typical of close-packed systems.[19,29] The peak around 0.5 (corresponding to the θ angle of 60°) clearly refers to close packed units of the structure, in which the three neighboring particles form an

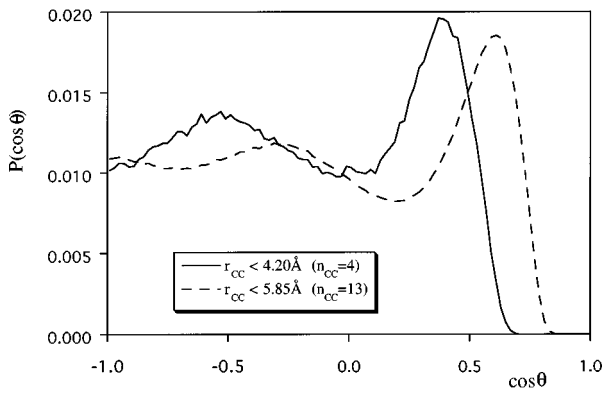

FIG. 7. Cosine distribution of the θ angle formed by two neighbor molecules around the central molecule.

equilateral triangle. The secondary peak of the distribution at -0.5, corresponding to the θ value of about 120°, is also the sign of this close-packed structure. The shift of the two peaks towards larger values with increasing number of neighbors taken into account refers simply to the fact that more distant neighbors can be located in similar directions from the central molecule than the closest ones (i.e., behind each other). The obtained distribution is markedly different from that of tetrahedrally packed systems, such as liquid water,[30] in which the main broad peak comes at about -0.25, the cosine value corresponding to the tetrahedral angle, and at 0.5 only a small second peak appears due to the off-network molecules.

The preferential location of the neighbor molecules around the central one has been investigated by projecting the position of the C atom of the neighbor molecules to the *XY*, *XZ*, and *YZ* planes of the central molecule-fixed coordinate frame. In defining this local coordinate frame the C atom of the central molecule has been chosen as the origin, the *X* axis corresponds to the main symmetry axis of the molecule (being the F atoms on its positive side), and the *XY* and *XZ* planes are the planes formed by its F–C–F and H–C–H atoms, respectively. The projection densities of the neighboring C atoms, which are closer to the origin than 3.8 Å (this C–C distance corresponds to the coordination num-

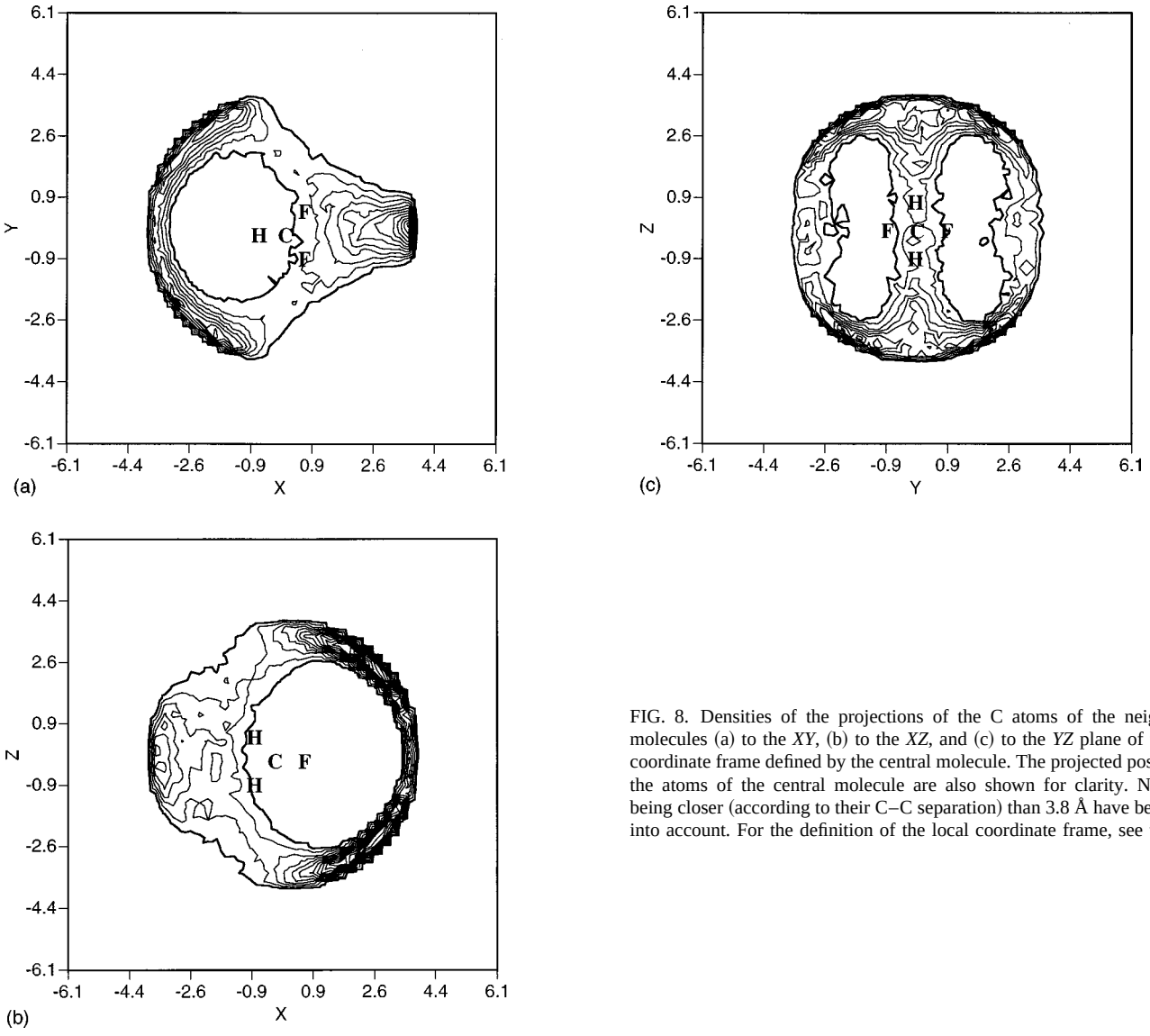

FIG. 8. Densities of the projections of the C atoms of the neighboring molecules (a) to the *XY*, (b) to the *XZ*, and (c) to the *YZ* plane of the local coordinate frame defined by the central molecule. The projected positions of the atoms of the central molecule are also shown for clarity. Neighbors being closer (according to their C–C separation) than 3.8 Å have been taken into account. For the definition of the local coordinate frame, see the text.

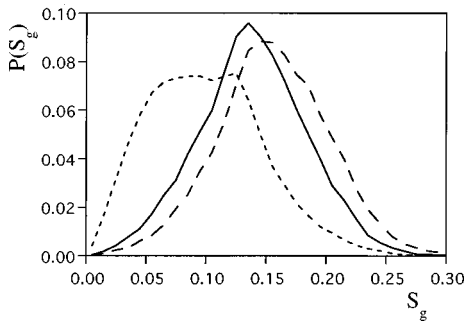

FIG. 9. Distribution of the S_g tetrahedral angular order parameter of the four nearest neighbors in liquid methylene fluoride (solid line). For comparison, its distribution in liquid argon (long dashes) and SPC water (short dashes) are also shown.

ber value of 1), are shown in Fig. 8. For clarity, the projected position of the atoms of the central molecule are also shown. As is evident from the *XY* and *XZ* projections, the neighbor molecules, such as in the case of the energy minimum dimers (see Fig. 1), are located towards the face centers of the tetrahedron of the central molecule. This preferential location of the neighbors is rather similar to that of other close-packed liquids of tetrahedral molecules, such as CH_2Cl_2 (Ref. 19) and CCl_4,[29] and is again in a clear contrast with liquid water,[31] where neighbors are located in the direction of the vertices (i.e., H atoms or lone pairs) instead of the face centers of the tetrahedron of the central molecule. The *YZ* projection shows that neighbors prefer to locate above and below the central molecule in planes parallel to its F–C–F plane, and also in the H–C–H plane of the central molecule. The former location would possibly involve antiparallel, whereas the latter head-to-tail type dipole–dipole arrangement. This point is discussed further in the following section.

As it has already seen from the analysis of the $P(\cos\theta)$ distribution, the preferential location of the neighbors in the direction of the face centers of the tetrahedron of the central molecule does not mean that the nearest neighbors are surrounding the central molecule tetrahedrally. In order to demonstrate this, we have calculated the distribution of the S_g tetrahedral angular order parameter as defined by Chau and Hardwick:[32]

$$S_g = \frac{3}{32}\sum_{i=1}^{3}\sum_{j=i+1}^{4}\left(\cos\psi_{ij}+\frac{1}{3}\right)^2. \tag{3}$$

Here indices i and j run through the four nearest neighbors and ψ_{ij} is the angle of the vectors pointing from the central particle towards the ith and jth neighbors (the position of the molecules have again been represented here by the position of their C atoms). The S_g order parameter is falling in the range of $0 \leqslant S_g \leqslant 1$, and its value is decreasing with increasing tetrahedrality of the arrangement of the four nearest neighbor molecules.

The obtained $P(S_g)$ distribution is shown in Fig. 9. For comparison, this distribution has also been calculated for liquid argon (using Lennard-Jones potential[33]) and for SPC[34] water. These distributions are also plotted in Fig. 9. As is evident, the present distribution is rather similar to that of liquid argon, it is only slightly shifted towards smaller values

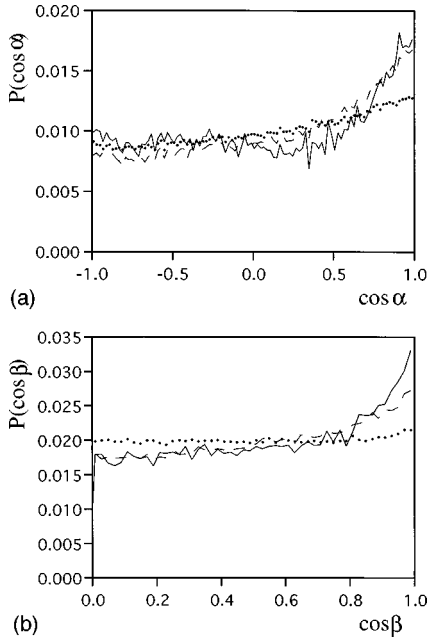

FIG. 10. (a) Cosine distribution of the dipole–dipole angle α and (b) the β angle formed by the F–C–F planes of the neighboring methylene fluoride molecules. Neighbors closer than 3.8 Å (solid lines), 4.2 Å (dashed lines) and 5.85 Å (dots) have been taken into account. Distances refer to C–C separation. The used maximum C–C distances correspond to 1, 4 and 13 neighbors in average, respectively.

(i.e., more tetrahedral arrangements). The mean value of the $P(S_g)$ distribution is resulted in 0.156 and 0.139 for liquid Ar and CH_2F_2, respectively. By contrast, the distribution for SPC water shows clearly higher tetrahedricity than the other two liquids, with $\langle S_g \rangle = 0.099$.

C. Relative orientation of the nearest neighbor molecules

1. Angular distributions

Similarly to the analysis of the nearest neighbor contributions to the partial pair correlation functions, we have also followed two different ways in the analysis of the preferential relative orientation of the nearest neighbor molecules, as they have been selected either by C–C or H–F separation. Thus Figs. 10(a) and 10(b) show the cosine distribution of the dipole–dipole angle α and the angle β formed by the F–C–F planes for molecular pairs of C–C separation smaller than 3.8, 4.2, and 5.85 Å (corresponding to the C–C coordination numbers of 1, 4, and 13, respectively). It turns out that the dipole moments of the nearest neighbors have a slight preference for antiparallel and a strong preference for parallel alignment. The former preference, which is consistent with the B-type energy minimum dimer arrangement (see Fig. 1), vanishes rapidly, and it is not present when the first four neighbors are taken into account. On the other hand, the preference of the parallel alignment is valid for a much longer distance range, it is extended to the entire first coordination shell. Contrary to the dipole vectors, the relative orientation of the F–C–F planes of the molecules are only correlated for the nearest C–C neighbors. These neighbors prefer parallel F–C–F alignment, again in agreement with

the B-type energy minimum dimer configuration. Taking the four nearest neighbors into account already a considerably weaker preference can be found, whereas the distribution obtained for all the first coordination shell molecules is almost completely uniform. The two distributions do not show any particular preference for the A-type (global) energy minimum dimer arrangement. Such a preference would involve a peak at about -0.28 on the $P(\cos\alpha)$ and at 0 on the $P(\cos\beta)$ distribution, however, these features are completely absent even on the distributions given by the closest neighbors.

The obtained dipole–dipole cosine distributions $P(\cos\alpha)$ are rather unusual for aprotic dipolar liquids. Liquids belonging to this group usually prefer antiparallel nearest neighbor dipole arrangement[14,18,19,24,25,35] (although in the case of CH_2Cl_2 a slight parallel preference has also been observed[19]). The antiparallel dipole–dipole orientation usually characterizes neighbors arranged in parallel planes above each other. Such an arrangement, which is typical for aprotic dipolar liquids,[14,18,19,24,35] is usually favored both by steric and electrostatic interactions. On the other hand, acute neighbor dipole–dipole angles are usually preferred in hydrogen bonded liquids of small molecules (e.g., water,[20,36] methanol,[37] or HF[38]). Since these molecules can rotate freely around the hydrogen bonds, this arrangement usually does not involve any preference for the plane–plane arrangement.[11] In a nonhydrogen bonding liquid, the preference for the parallel orientation of the neighbor dipole moments indicates head-to-tail type arrangement. Thus, the observed slight and short ranged preference for antiparallel dipole–dipole and parallel plane–plane orientations can correspond to neighbors of orientation typical of aprotic dipolar liquids (such as dimer B in Fig. 1), whereas the strong preference of parallel alignment of the neighboring dipoles indicate either the presence of hydrogen bonding or simple head-to-tail nearest neighbor arrangement. The fact that this correlation extends to the entire first coordination shell of 13 neighbors in average, in agreement with our previous findings, suggests the predominance of the latter orientation, as orientational correlations due to hydrogen bonding are usually short ranged covering only the hydrogen bonded neighbors themselves.[20,28,30,36]

In investigating the relative orientation of the close H–F contact neighbors, we have also calculated the cosine distributions of their C–H$\cdots$F angle γ and the angle of their F–C–F planes. The results are shown in Fig. 11. Here we have taken into account neighbors having a H$\cdots$F contact closer than 3.55 Å, the position of the first minimum of the $g_{HF}(r)$ partial pair correlation function. The two cosine distributions have then been recalculated with the combined criterion of the H$\cdots$F contact being closer than 3.55 Å and the corresponding C$\cdots$F distance smaller than 4.0 Å. However, the latter criterion does not have considerable effect as the results obtained with and without this additional criterion are almost equivalent. The obtained cosine distribution of the C–H$\cdots$F angles is remarkably different from the similar distribution of hydrogen bonded liquids. The preferential arrangement of the hydrogen bond is always linear, even for weak hydrogen bonds like in the case of supercritical water[39]

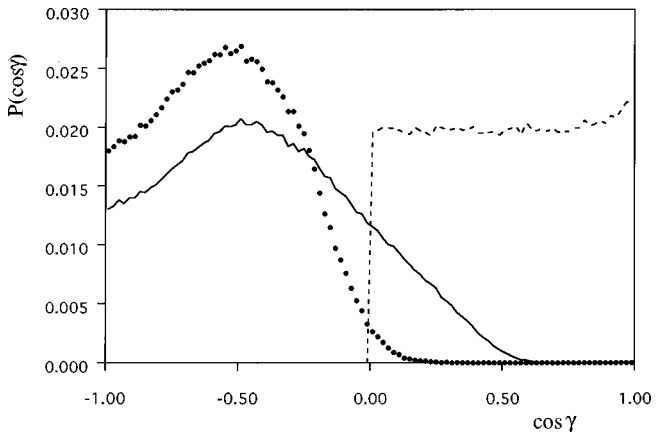

FIG. 11. Cosine distribution of angles characterizing the relative orientation of close H–F contact molecular pairs. H–F pairs closer than 3.55 Å are regarded to be close contact. Solid line: C–H$\cdots$F angle, taking every close H–F contact into account. Dots: C–H$\cdots$F angle, taking only the closest H–F pair into account for molecular pairs having more than one close H–F contact. Dashed line: angle formed by the two F–C–F planes.

or the C–H$\cdots$O type hydrogen bonds present in liquid formic acid,[11] when only the strength of this preference becomes weaker than for strong hydrogen bonds. However, the present distribution has its peak at about -0.5, corresponding to a C–H$\cdots$F angle of 120 °, which agrees well with the value of 130 ° estimated from the positions of the first peak of $g_{HF}(r)$ and $g_{CF}(r)$ (see Sec. V A). Since in this analysis, every C–H$\cdots$F angle corresponding to close contact H–F pairs have been taken into account, a pair of molecules could have contributed to the distribution with more than one angle (i.e., two molecules may have more than one close contact H–F pairs). In order to demonstrate that the observed behavior of the $P(\cos\gamma)$ distribution is not simply a feature introduced by these multiple contributions of some molecular pairs, we have recalculated the present distribution taking only the nearest H–F pairs into account for neighbors of multiple H–F contact. However, as shown in Fig. 11, the obtained distribution is rather similar to that of every close contact H–F pairs, its maximum being at almost the same position. It means that the observed preference of the C–H$\cdots$F angle for being about 120° is rather general, it is followed by the closest contact H–F pairs as well as by more distant ones belonging still to the first peak region of $g_{HF}(r)$. The observed behavior of the obtained $P(\cos\gamma)$ distributions excludes extensive C–H$\cdots$F type hydrogen bonding, whereas it is consistent with the presence of neighbors having more than one close H–F contacts, such as in any kind of head-to-tail type arrangements, which appears to be the dominant structural element of liquid methylene fluoride. It is also evident from Fig. 11. that the alignment of the F–C–F planes of these close H–F contact molecular pairs do not prefer any particular angle, the corresponding cosine distribution is uniform, indicating that these close H–F contact head-to-tail type neighbours can freely rotate around their dipolar axes.

2. Spherical harmonic coefficient analysis

The orientational correlation of the molecules can fully be characterized by the $g(r,\omega_1,\omega_2,\omega)$ orientational pair correlation function, where $\omega_i=(\phi_i,\vartheta_i,\chi_i)$ are the Euler angles describing the orientation of the ith molecule ($i=1$ or 2), and $\omega=(\vartheta,\phi)$ are the angular polar coordinates of the center of the second molecule in a space-fixed coordinate frame in which the center of the first molecule defines the origin. Fixing the z axis of this frame along the vector joining the two molecular centers ω can be eliminated. In this coordinate frame the orientational pair correlation function can be expanded in a series as[13,40]

$$g(r,\omega_1,\omega_2)=\sum_{l_1l_2l}\sum_{n_1n_2} g_{l_1l_2l,n_1n_2}(r)\Phi_{l_1l_2l,n_1n_2}(\omega_1,\omega_2), \tag{4}$$

where the ranges of the indices are restricted to $l_1\geqslant 0$, $l_2\geqslant 0$ and $l_1+l_2\geqslant l\geqslant|l_1-l_2|$, the $g_{l_1l_2l,n_1n_2}(r)$ functions are the coefficients of the expansion, and the orientation dependent $\Phi_{l_1l_2l,n_1n_2}(\omega_1,\omega_2)$ function have the form

$$\Phi_{l_1l_2l,n_1n_2}(\omega_1,\omega_2)=\sum_{m=-\min(l_1,l_2)}^{\min(l_1,l_2)} C(l_1l_2l,m\underline{m}0) \times D^{l_1}_{mn_1}{}^*(\omega_1)D^{l_2}_{\underline{m}n_2}{}^*(\omega_2). \tag{5}$$

Here $C(l_1l_2l,m\underline{m}0)$ are the Clebsch–Gordan coefficients, $D^l_{mn}(\omega)$ is the generalized spherical harmonic of order mnl,[13] $\underline{m}=-m$ and asterisks denote complex conjugate. It should be noted that $g(r,\omega_1,\omega_2)$ is strictly a function of only six independent variables, since instead of ϕ_1 and ϕ_2 only $\Delta\phi=\phi_2-\phi_1$ is independent. Using the sum rules of the Clebsch–Gordan coefficients and the orthogonality properties of the $D^l_{mn}(\omega)$ spherical harmonics[13] Eq. (4) can be inverted and the coefficients of the expansion can be obtained as

$$g_{l_1l_2l,n_1n_2}(r)=(2l_1+1)(2l_2+1)g_{cc}(r) \times\langle\Phi^*_{l_1l_2l,n_1n_2}(\omega_1,\omega_2)\rangle_r. \tag{6}$$

Here $g_{cc}(r)$ is the center–center pair correlation function and the brackets $\langle\cdots\rangle_r$ denote ensemble averaging over the orientation of all molecular pairs separated by the center-center distance of r. It should be noted that Eq. (6) differs from the formula of Gray and Gubbins[13] by a factor of $[(2l+1)/4\pi]^{1/2}$, and thus $g_{000,00}(r)=g_{cc}(r)$ here. The explicit form of several leading terms of this expansion are given elsewhere.[28,36]

Some of the obtained $g_{l_1l_2l,n_1n_2}(r)$ coefficients of this spherical harmonic expansion of $g(r,\omega_1,\omega_2)$ are summarized in Fig. 12 as obtained from the present simulation. The $g_{000,00}(r)$ function is identical with the center of mass-center of mass pair correlation function and thus it is rather similar to $g_{CC}(r)$. Indeed, the position of all the minima and maxima of $g_{000,00}(r)$ agrees within 0.2 Å with that of $g_{CC}(r)$, and the integration of the first peak of $g_{000,00}(r)$ up to the first minimum gives also a coordination number of 13. The analysis of the higher order coefficients, which represent real orientational correlation, can confirm our above findings

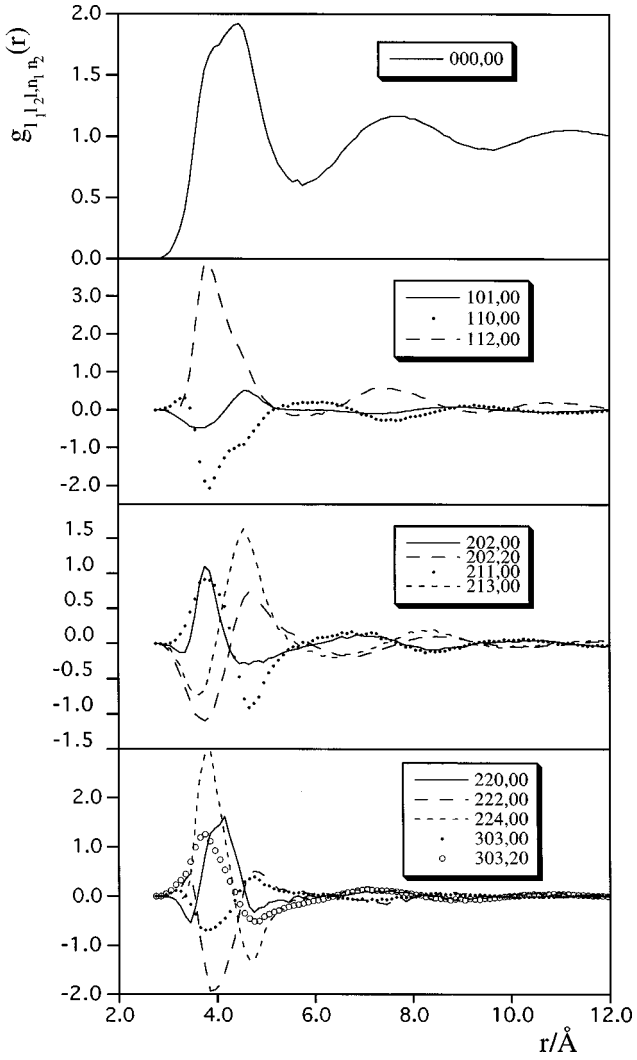

FIG. 12. Several coefficients of the spherical harmonic expansion [Eq. (4)] of the orientational pair correlation function of liquid methylene fluoride as obtained from the present simulation.

on the preferential orientation of the molecules. The shape of the obtained coefficients is rather similar to that of liquid CH_2Cl_2 (see Fig. 9. of Ref. 19), indicating that the orientational correlation of the molecules are rather similar in the two liquids. The main negative peak of $g_{110,00}(r)$ below 4 Å is a clear indication of the preferential head-to-tail arrangement of the neighbours of this distance, since this coefficient is proportional to $-\langle\cos\alpha\rangle_r$ being α the dipole–dipole angle of the two molecules.

Information on the strength of the orientational correlation of the molecules can be obtained from the amplitude of the peaks and minima of the $g_{l_1l_2l,n_1n_2}(r)$ coefficients. When comparing these amplitudes with those in liquid H_2S,[18] CH_2Cl_2,[19] and water,[36] i.e., a weakly dipolar, a strongly dipolar and a hydrogen bonding representative of the C_{2v} symmetry group, it turns out that the short-range orientational order in liquid CH_2F_2 is about as strong as in liquid water and considerably stronger than in CH_2Cl_2.[41] The obtained $g_{l_1l_2l,n_1n_2}(r)$ coefficients show noticeable oscillations up to 10 Å, indicating that the orientational correlation of the molecules is extended up to the end of the second coordination

shell, and thus it involves about 60 neighbors. This relatively long range of the existence of orientational correlation, which has also been observed in liquid methylene chloride,[19] is in a clear contrast with strongly hydrogen bonded liquids, where orientational correlation is usually extended only to the few hydrogen bonded neighbors and vanishes beyond them.[28,30,36] This fact underlines again that the relative orientation of the neighboring molecules in liquid methylene fluoride is determined mainly by dipole–dipole and not by hydrogen bonding interactions.

VI. CONCLUSIONS

In this work, the structure of liquid methylene fluoride has been analyzed in detail on the basis of Monte Carlo simulation results. For this purpose, we have modified the Potter–Tildesley–Burgess–Rogers potential model. The new model is able to reproduce the important thermodynamic parameters (internal energy, density, heat capacity), the vapor-liquid equilibrium, and the experimental structure of the system with considerably better accuracy than the previous models. As is usual in computer simulation studies, this good reproduction of a set of different physical properties can give one some confidence in the results of the following detailed analysis. Obviously, the model could also have been tested against several other physical properties (e.g., diffusion coefficient, dielectric constant, free energy, etc.). A possible good reproduction of these quantities would give further support of the reliability of this model. Work in this direction is currently in progress.

It has turned out from the analysis of the nearest neighbor structure that although nearest neighbors are located preferentially towards the face centers of the tetrahedron of the central molecule, there is no particular tetrahedral ordering present in liquid methylene fluoride. The molecules form closely packed structure, such as in simple liquids like argon.

It has been found that the most preferred alignment of the nearest neighbors is a head-to-tail type arrangement. This preferential orientation is clearly a consequence of entropic effects, since this arrangement does not correspond to any local minimum on the dimer potential energy surface of the potential model. On the other hand, no preference has been found in the liquid phase for the dimer structure corresponding to the global minimum of this surface. Slight preference has been observed for the other minimum energy dimer arrangement, in which the F–C–F planes of the molecules are parallel and their dipole vectors form an angle of 180°. Similar orientational preferences have been found in liquid CH_2Cl_2,[19] however, there the relative importance of the head-to-tail type arrangements were found to be considerably smaller, whereas that of the antiparallel dipole–dipole orientation fare greater than here. Similarly to liquid methylene chloride, close H–H contact neighbors have also been observed here, although in a much smaller extent. This kind of arrangement is clearly preferred by steric and disfavored by electrostatic interactions, and thus the relative importance of such neighbors is larger when the size of the halogen atoms is larger and the dipole moment of the molecules is smaller.

In analyzing the nearest neighbor structure no evidence has been found for C–H$\cdots$F type hydrogen bonding between the molecules. Obviously, it is hard to distinguish between head-to-tail type nearest neighbor arrangements with close H–F contacts and weak hydrogen bonds with distorted geometry on the basis of a classical simulation. However, several observations, such as the large coordination number of the first peak of $g_{HF}(r)$; the position of this peak being only at 2.55 Å [by contrast, in liquid HF the position of the hydrogen bonding peak of $g_{HF}(r)$ appears at about 1.5 Å[28,38]]; the most probable C–H$\cdots$F angle of close contact H–F pairs being about 120 ° rather than linear; and the fact that the range of the existing orientational correlation of the molecules is rather large extending even to the second coordination shell suggest that strong dipole–dipole rather than exceptionally weak hydrogen bonding interactions are dominating in liquid methylene fluoride.

ACKNOWLEDGMENTS

The authors are grateful to Dr. Karsten Meier (Hannover University, Germany) for providing the computer code for the Tillner–Roth–Yokozeki equation of state and to draw this equation of state to our attention. One of the authors (P.J.) is supported by the Hungarian Ministry of Culture and Education as an Eötvös fellow and by the Hungarian Soros Foundation, Budapest, which is gratefully appreciated.

[1] C. Vega, B. Saager, and J. Fischer, Mol. Phys. **68**, 1079 (1989).
[2] R. Yamamoto, O. Kitao, and K. Nakanishi, Mol. Simul. **12**, 383 (1994).
[3] R. Yamamoto, O. Kitao, and K. Nakanishi, Fluid Phase Equilibria **104**, 349 (1995).
[4] M. Lisal and V. Vacek, Mol. Phys. **87**, 167 (1996).
[5] K. A. Mort, K. A. Johnson, D. L. Cooper, A. N. Burgess, and W. S. Howells, Mol. Phys. **90**, 415 (1997).
[6] S. Higashi and A. Takada, Mol. Phys. **92**, 641 (1997).
[7] S. C. Potter, D. J. Tildesley, A. N. Burgess, and S. C. Rogers, Mol. Phys. **92**, 825 (1997).
[8] L. Turi and J. J. Dannenberg, J. Phys. Chem. **97**, 7899 (1993).
[9] I. Alkorta and S. Maluendes, J. Phys. Chem. **99**, 6457 (1995).
[10] P. Jedlovszky and L. Turi, J. Phys. Chem. A **101**, 2662 (1997).
[11] P. Jedlovszky and L. Turi, J. Phys. Chem. B **101**, 5429 (1997).
[12] L. Turi, Chem. Phys. Lett. **275**, 35 (1997).
[13] C. G. Gray and K. E. Gubbins, *Theory of Molecular Fluids, Vol. 1: Fundamentals* (Clarendon, Oxford, 1984).
[14] T. Radnai, I. Bakó, P. Jedlovszky, and G. Pálinkás, Mol. Simul. **16**, 345 (1996).
[15] K. A. Mort, Ph.D. thesis, University of Liverpool, 1998; K. A. Mort, K. A. Johnson, A. N. Burgess, W. S. Howells, and D. L. Cooper (unpublished).
[16] R. Tillner-Roth and A. Yokozeki, J. Phys. Chem. Ref. Data **26**, 1273 (1997).
[17] *Water-A Comprehensive Treatise*, edited by F. Franks (Plenum, New York, 1972–1979), Vols. 1–8.
[18] P. Jedlovszky, Mol. Phys. **93**, 939 (1998).
[19] P. Jedlovszky, J. Chem. Phys. **107**, 562 (1997).
[20] J. A. Barker and R. O. Watts, Mol. Phys. **26**, 789 (1973).
[21] M. Neumann, J. Chem. Phys. **82**, 5663 (1985).
[22] M. P. Allen and D. J. Tildesley, *Computer Simulation of Liquids* (Oxford University Press, Oxford, 1987).
[23] P. F. Malbrunot, P. A. Meunier, G. M. Scatena, W. H. Mears, K. P. Murphy, and J. V. Sinka, J. Chem. Eng. Data **13**, 16 (1968).
[24] P. Jedlovszky and G. Pálinkás, Mol. Phys. **84**, 217 (1995).
[25] W. L. Jorgensen and J. M. Briggs, Mol. Phys. **63**, 547 (1988).
[26] A. Z. Panagiotopoulos, Mol. Phys. **61**, 813 (1987).
[27] M. Mezei, Mol. Phys. **40**, 901 (1980).
[28] P. Jedlovszky and R. Vallauri, Mol. Phys. **93**, 15 (1998).
[29] P. Jedlovszky, J. Chem. Phys. **107**, 7433 (1997).
[30] P. Jedlovszky, I. Bakó, G. Pálinkás, T. Radnai, and A. K. Soper, J. Chem. Phys. **105**, 245 (1996).

[31] P. Jedlovszky, I. Bakó, and G. Pálinkás, Chem. Phys. Lett. **221**, 183 (1994).
[32] P. L. Chau and A. J. Hardwick, Mol. Phys. **93**, 511 (1998).
[33] I. Ruff, A. Baranyai, G. Pálinkás, and K. Heinzinger, J. Chem. Phys. **85**, 2169 (1986).
[34] H. J. C. Berendsen, J. P. M. Postma, W. F. von Guntseren, and J. Hermans, in *Intermolecular Forces*, edited by C. Pullman (Reidel, Dordrecht, 1981).
[35] I. Bakó, T. Radnai, and G. Pálinkás, Z. Naturforsch., A: Phys. Sci. **51**, 859 (1996).
[36] H. Xu and M. Kotbi, Chem. Phys. Lett. **248**, 89 (1996).
[37] G. Pálinkás, E. Hawlicka, and K. Heinzinger, J. Phys. Chem. **91**, 4334 (1987).
[38] P. Jedlovszky and R. Vallauri, J. Chem. Phys. **107**, 10166 (1997).
[39] P. Jedlovszky, J. P. Brodholt, F. Bruni, M. A. Ricci, A. K. Soper, and R. Vallauri, J. Chem. Phys. **108**, 8528 (1998).
[40] L. Blum and A. J. Torruela, J. Chem. Phys. **56**, 303 (1972).
[41] Note that in Ref. 19 slightly different convention was used than here, and thus the coefficients shown in Fig. 9 of Ref. 19 should be divided by $[(2l+1)/4\pi]^{1/2}$ to be comparable with the present ones.